

ELECTRON COOLING AT INS-TARN II

T. Tanabe, T. Honma, M. Sekiguchi, H. Tsujikawa, A. Mizobuchi, T. Oosuga,
M. Kodaira, M. Takanaka, M. Kanazawa, A. Noda, K. Sato, I. Sugai and M. Yasue
Institute for Nuclear Study, University of Tokyo,
Tanashi, Tokyo 188, Japan

Summary

The construction of an electron-cooling device is now in progress. The ion beam accelerated and stored in a ring TARN II is cooled by the device with the maximum electron energy of 120 keV and the maximum current density of 0.5 A/cm². Design and status of each element of the cooling system are described. Results of the feasibility study of a microparticle internal target are also presented.

General Description of the Project

The construction of a synchrotron-cooler ring TARN II is currently in progress. The maximum energies of this machine are 1 GeV for proton and 340 MeV/u for heavy ions with charge to mass ratio of 1/2. The ring consists of 78 m circumference with regular hexagonal layout. Beams including heavy ions up to neon are injected from an existing sector focusing cyclotron with K-number of 68. A new feature of this machine is that the phase space density of the stored ion beam is compressed by using an electron cooling device. This can cool ion beams up to 200 MeV/u. The electron cooling project primarily aims at the studies of the cooling technique itself. The cooled good quality beam will also be used for the studies of atomic and nuclear physics in future. Relating to the application of

the machine, a feasibility study of an internal target has been started. Among many candidates for the internal target, a microparticle target was chosen for the study since only a few studies have been made on the target for solid substances. The results of the studies made so far on the cooling project appeared in refs. 1 ~ 3.

Electron Cooling System

General

The main parameters of the electron cooling system are listed in Table 1. The length of the cooling section of 1.5 m is limited by the length of the straight section of the ring which is 4.2 m. The diameter of the electron beam is 50 mm and the maximum current density is 0.5 A/cm². The layout of the cooling device is shown in Fig. 1. The electron beam is injected and ejected over the beam line of the TARN II ring. In order to make the maintenance work easy, the whole system is mounted on a wheeled base which is movable along a pair of rails. The high voltage system to accelerate electrons is installed just next to the cooling device to reduce the length of the high voltage cable. The orbit deformation of the ion beam due to the toroids is corrected by two pairs of steering dipoles at both ends of the cooling device.

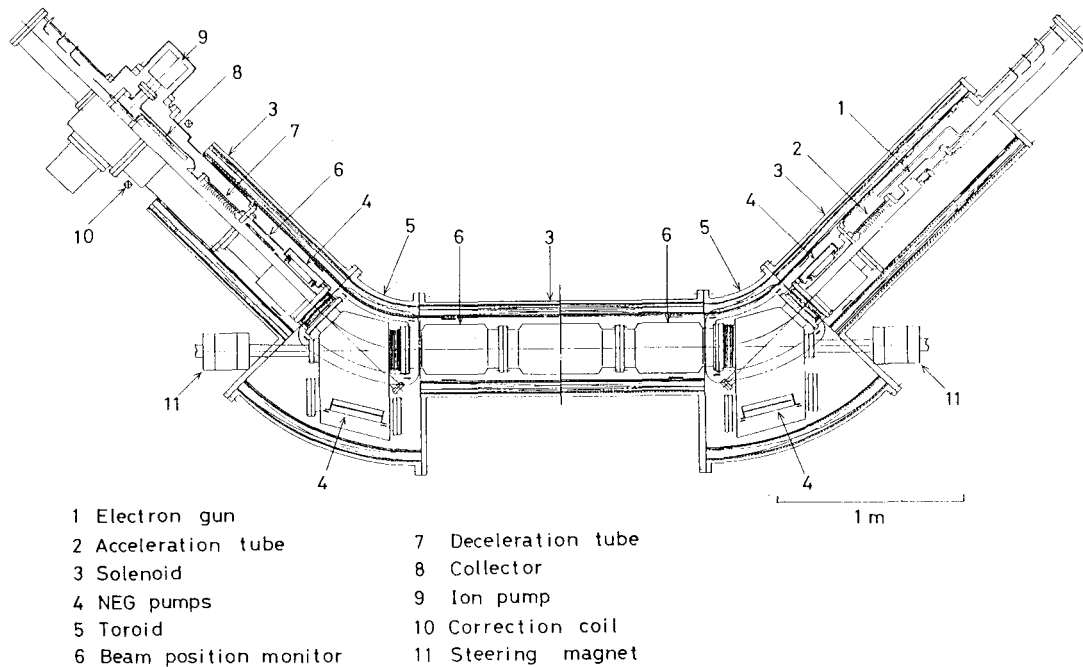


Fig. 1. Layout of electron cooling device.

Table 1. Electron cooling parameters

Maximum working energy	ion	200 MeV/u
	electron	120 keV
Cooled ions		$H^+ - 20Ne^{10+}$
Length of interaction region		1.5 m
Maximum electron current density		0.5 A/cm ²
Cathode diameter		50 mm
Maximum electron current		10 A
Maximum solenoid field		1.2 kG
Electron gun perveance		1.0 $\mu A/V^{3/2}$

Electron Optics

A flat electron gun is surrounded by the Pierce electrode to minimize the transverse electric field components. Electrons emitted from the cathode are extracted by the gun anode high voltage and are further accelerated up to full energies by the grading potential acceleration column. The whole system is immersed in a uniform solenoid field. Transverse electron temperature depends on the position and the shape of the anode and furthermore on the solenoid field. The electron temperature in the gun region is studied with the help of SLAC program⁴. An example of the electron trajectories is shown in Fig. 2. Outermost electrons generally have the highest transverse temperature. The maximum solenoid field of 1.2 kG is high enough to reduce the temperature to less than 0.1 eV.

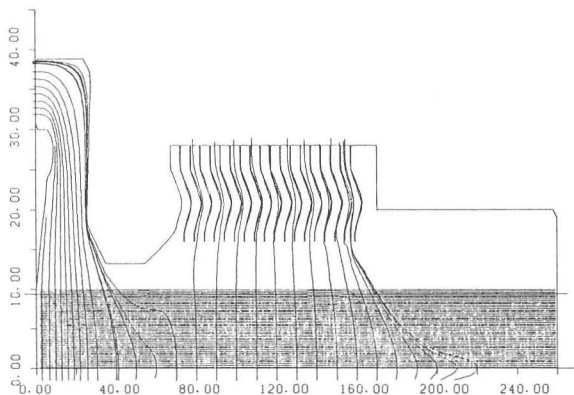


Fig. 2. Calculated electron trajectories in the gun region. Electrons are accelerated to 110 keV at the solenoid field of 1.06 kG. The electron current is 10 A.

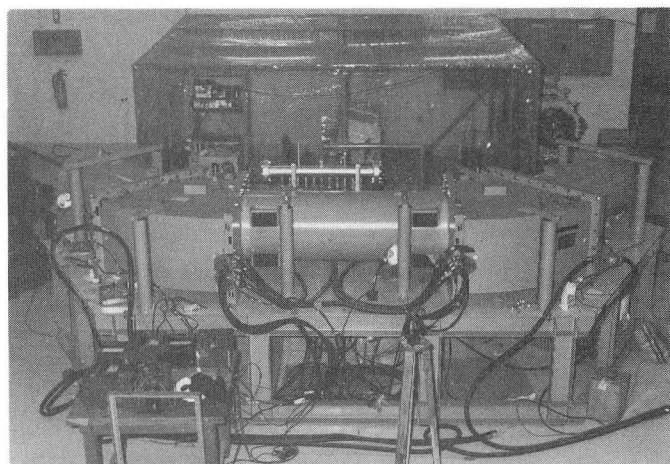


Fig. 3. Electron guiding solenoids and toroids.

Electron Guiding Coils

Figure 3 shows a photograph of the magnet system. The main components of the electron guiding coils are three solenoids with inner diameter of 36 cm and two 45°-toroids. The diameter of the solenoid is minimum size to hold the high voltage of 120 kV stably in the gun and collector vessels. Solenoid and toroid coils are connected in series to the same power supply. Only outermost coils of both toroids are excited by another power supply and the correct fraction of the current was found with the help of the field measurements. In order to realize the uniform field along the electron path, several correction coils are installed at the electron gun region to correct the gradually decreasing field inside the solenoid end and at each connecting part between solenoid and toroid to compensate the field discontinuity. At the collector end, a pair of correction coils are added to form the decreasing axial field. Furthermore correction coils producing homogeneous transverse field over the electron beam are wound on to the outer surface of the solenoids and toroids. They can change the field direction in order to steer the electron beam or to cancel the drift motion due to the centrifugal force in the toroids. The solenoids and the toroids are surrounded by soft iron shieldings 15 mm thick except the windows needed for the passage of electrons and ions.

The three components of the magnetic field were measured with high precision by using three Hall plates (Siemens SBV601). They are fixed to the end of a stainless steel arm of 3 m in length which can be moved by the scanning device along three orthogonal axes. The resolution of the Hall voltage measurement and the stability of the measuring electronics system are of order of 10^{-4} for the full field. The results of the field measurements are shown in Fig. 4. A good quality field has been achieved for the cooling solenoid.

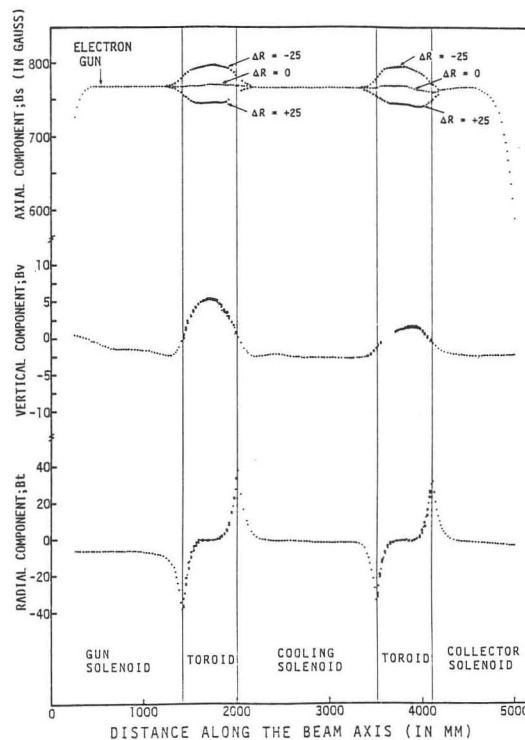


Fig. 4. Magnetic field components of the electron guiding coils. The fields off the axis by ± 25 mm as well as those on the axis are shown.

High Voltage System

The high voltage system for the electron cooling consists of a high voltage power supply (HVPS) for the acceleration and the deceleration of electrons (120 kV-20 mA), a gun anode PS (50 kV-20 mA), a collector PS (6 kV-10 A) and a collector anode PS (6 kV-20 mA). All the power supplies except the HVPS are housed in a high voltage platform with the maximum voltage of 120 kV. Figure 5 shows a photograph of the high voltage system. The good stability of the HVPS is essential to obtain the low longitudinal electron temperature. The stability of $+ 1 \times 10^{-5}$ has already been achieved at 120 kV. The space charge due to the high density electron beam gives rise to an unwanted tune shift, especially for the low energy ions during injection and acceleration. In order to suppress the electron current for low energy ions, the gun anode PS is designed to allow fast switching (1 ms) of the electron beam synchronized with the cycling of the TARN II.

Vacuum Chamber

Figure 6 shows a photograph of the vacuum chamber. It consists of several stainless steel (SUS 316L) vessels and is bakeable to 350 °C. Vacuum is attained by using four groups of non-evaporable getter pumps (Saes St 707) installed close to the cathode and the collector and also inside both toroid chambers. Total pumping speed amounts to about 8000 l/s for H₂ at room temperature. Inside the vacuum chamber we have drift tubes, electrostatic position monitor electrodes and antennas to pick up microwave emitted by the spiral motion of electrons in the magnetic field.

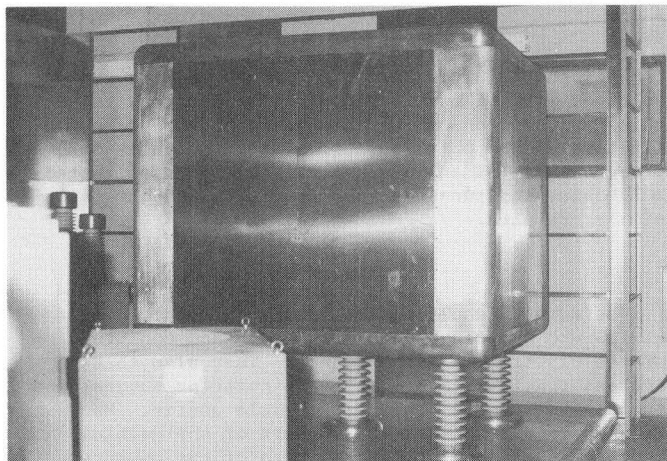


Fig. 5. High voltage platform and power supplies for the electron cooling system.

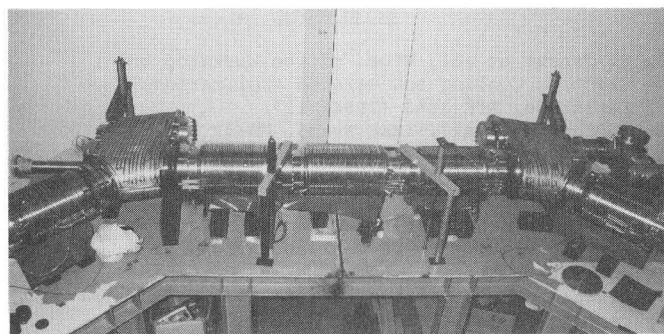


Fig. 6. Vacuum chamber for the electron cooling system.

Measurements with Small Electron Beam

The electron trajectory on the axis was actually traced using a small electron beam of about 0.5 mm in width. A small electron gun with the acceleration voltage of 6 kV was installed on the axis of the gun solenoid. The electron path starting from the gun and ending in the collector was visually observed by viewing the light emitted from the Y₂O₃ coated glass plates due to the electron bombardment. Inside the central solenoid the plate was moved along the axis and the electron position was identified by a telescope fixed to a milling machine table. Figure 7 shows the trajectories of electrons through the cooling solenoid. The fraction of deviation less than about $+ 2 \times 10^{-4}$ ranging over 1.2 m is consistent with the results of the magnetic field measurements.

Simulation of the Cooling Process

Electron cooling process was simulated assuming realistic conditions for the ring and the electron cooling device with the help of a program SPEC⁵. A typical example is shown in Fig. 8. The cooling time of a few seconds can be expected. The time dependence of the beam emittance and momentum width during the cooling was studied also for various ring lattice parameters, number of stored particles and electron current densities⁶. Studies on the optimization of lattice parameters have to be continued also taking account of the beam heating due to the internal target. A possible way to cool down hot beam with large longitudinal temperature was studied and it has been shown that the hot beam can be cooled in a short time if we sweep electron energy dynamically with a suitable speed⁶.

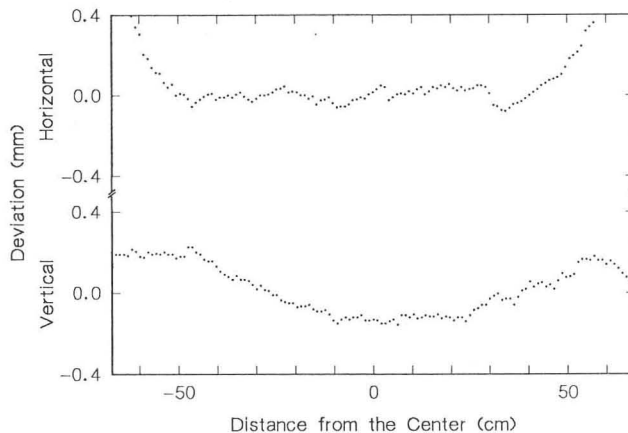


Fig. 7. Deviation of electron trajectories in the cooling region.

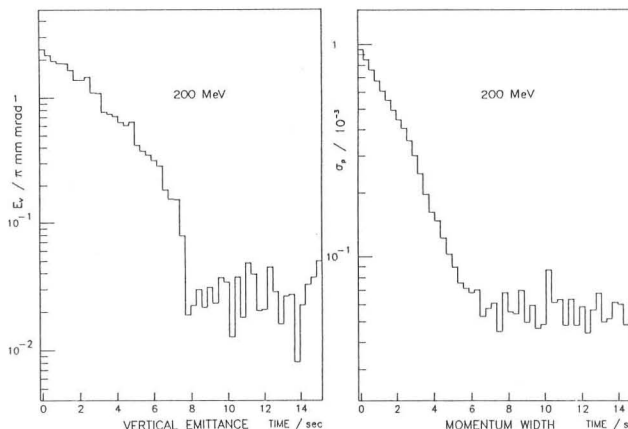


Fig. 8. Time dependence of emittance and momentum width of cooled ions after injection.

Internal Target

The use of the cooler ring with an internal target is very attractive for the studies of the nuclear physics, because high resolution studies are possible at a reasonable luminosity under the balance between the beam heating caused by the internal target and the beam cooling using the low temperature electrons. We have started the studies of the internal target. Among many candidates for the internal target⁷, a microparticle target was adopted for a feasibility study⁸, because microparticles are available for most solid materials and the apparatus can be made inexpensively.

The principle of the charged microparticle flux production is described as follows: When a dc high voltage is applied between two parallel-plate electrodes, microparticles scattered on the lower plate are contact-charged and repelled up to the upper plate, where they change their charge to an opposite sign and are accelerated back to the lower plate. In this way, they move up and down between these plates. These moving particles can be extracted through a hole in the upper plate and be accelerated up to the energies determined by the accelerating electrode. Then they are brought to the target region being focused by the einzel lenses. A picture of the target used for the present test is shown in Fig. 9.

The target thickness was estimated by measuring elastically scattered ions. In the experiments, nickel microparticles of 1 μm in average diameter are negatively charged and are accelerated at about 4 kV. Negative charge is preferable for the internal target, since positively charged particles are repelled by the ion beam space charge at the intersection region⁷. The particle flux with 4 mm in diameter was then bombarded perpendicularly by 65 MeV alpha-beam from the INS-SF cyclotron and the elastically scattered particles were detected at 11°. The yields were compared with those measured under the same conditions for a nickel foil of 1 mg/cm² in thickness. Figure 10 shows the target thickness as a function of the ion source voltage.

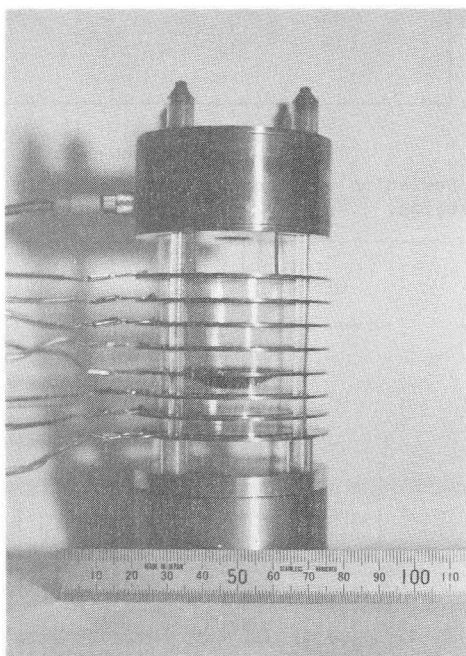


Fig. 9. Microparticle source used for the test.

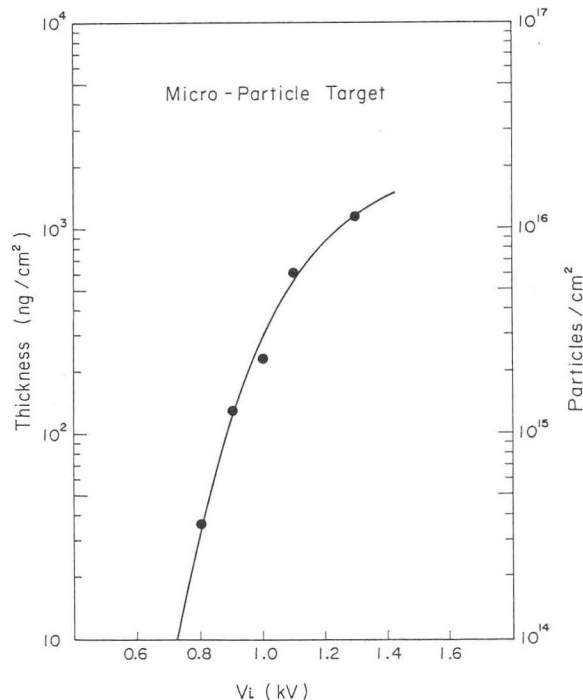


Fig. 10. Thickness of the microparticle target as a function of the source voltage.

The thickness is controllable by changing the source voltage. The allowable range of the internal target thickness depends on the luminosity and the beam lifetime⁹. The observed thickness is suitable for practical use as an internal target. We also tested molybdenum and tungsten microparticles and obtained similar results.

Acknowledgements

The authors would like to thank all of the staff at INS who contributed to the design and construction of the electron cooling project. They also thank Professor F. Fukuzawa for his stimulating suggestions and discussions on the microparticle source. Many thanks are also due to the members of the machine shop for their support and members of the computer section for the use of the FACOM M-380 computer. The electron cooling project was supported by the Grant for Scientific Research of the Ministry of Education.

References

1. T. Tanabe et al., Proc. of the Workshop on Electron Cooling and Related Applications, Karlsruhe, KfK 3846 (1984) 127.
2. T. Tanabe et al., IEEE Trans. NS-32 (1985) 2412.
3. T. Tanabe, Proc. of the 13th Int. Conf. on High Energy Accelerators, Novosibirsk (1986), to be published.
4. W. B. Herrmansfeldt, SLAC Report 226 (1979).
5. H. Poth et al., to be published in Nucl. Instr. and Meth..
6. T. Tanabe et al., Institute for Nuclear Study report INS-T-454 (1986).
7. H. O. Meyer, Proc. of the CEBAF Workshop (1985).
8. T. Tanabe, I. Sugai and M. Yasue, to be published.
9. H. O. Meyer, Nucl. Instr. and Meth. B10/11 (1985) 342.